1521-009X/49/2/121–132$35.00
Drug Metabolism and Disposition

https://doi.org/10.1124/dmd.120.000246
Drug Metab Dispos 49:121–132, February 2021

In Vitro Metabolism of Slowly Cleared G Protein–Coupled Receptor 139 Agonist TAK-041 Using Rat, Dog, Monkey, and Human Hepatocyte Models (HepatoPac): Correlation with In Vivo Metabolism

Amin Kamel, Steve Bowlin, Natalie Hosea, Dimitrios Arkilo, and Antonio Laurenza

Global Drug Metabolism and Pharmacokinetics, Takeda California Inc., San Diego, California (A.K., S.B., N.H.) and Clinical and Neuroscience Therapeutic Area, Takeda Boston Inc., Boston, Massachusetts (D.A., A.L.)

Received September 9, 2020; accepted November 24, 2020

ABSTRACT

Hepatic metabolism of low-clearance compound TAK-041 was studied in two different in vitro model systems using rat, dog, monkey, and human suspended cryopreserved hepatocytes and HepatoPac micropatterned coculture model primary hepatocytes. The aim of this work was to investigate the most appropriate system to assess the biotransformation of TAK-041, determine any notable species difference in the rate and in the extent of its metabolic pathways, and establish correlation with in vivo metabolism. TAK-041 exhibited very low turnover in suspended cryopreserved hepatocyte suspensions for all species, with no metabolites observed in human hepatocytes. However, incubations conducted for up to 14 days in the HepatoPac model resulted in more robust metabolic turnover. The major biotransformation pathways of TAK-041 proceed via hydroxylation on the benzene ring fused to the oxotriazine moiety and subsequent sulfate, glucuronide, and glutathione conjugation reactions. The glutathione conjugate of TAK-041 undergoes further downstream metabolism to produce the cysteine S-conjugate, which then undergoes *N*-acetylation to mercapturic acid and/or conversion to β-lyase–derived thiol metabolites. The minor biotransformation pathways include novel ring closure and hydrolysis, hydroxylation, oxidative *N*-dealkylation, and subsequent reduction. The HepatoPac model shows a notable species difference in the rate and in the extent of metabolic pathways of TAK-041, with dogs having the fastest metabolic clearance and humans the slowest. Furthermore, the model shows its suitability for establishing correlation with in vivo metabolism of low-turnover and extensively metabolized compounds such as TAK-041, displaying an extensive and unusual downstream sequential β-lyase–derived thiol metabolism in preclinical species and human.

SIGNIFICANCE STATEMENT

This study investigated the most appropriate in vitro system to assess the biotransformation of the low-turnover and extensively metabolized compound TAK-041, determine any notable species difference in the rate and in the extent of its metabolic pathways, and establish correlation with in vivo metabolism. The HepatoPac model was identified and showed its suitability for species comparison and establishing correlation, with in vivo metabolism displaying an extensive and unusual downstream sequential β-lyase–derived thiol metabolism in preclinical species and human.

Introduction

TAK-041 [(*S*)-2-(4-oxobenzo[d][1,2,3]triazin-3(4H)-yl)-*N*-(1-(4-(trifluoromethoxy)phenyl)ethyl)acetamide] is a first-in-class, potent, and selective small-molecule G protein–coupled receptor 139 (GPR139) agonist that is being developed for treating cognitive impairment and negative symptoms associated with schizophrenia. GPR139 is almost exclusively expressed in the central nervous system (Gloriam et al., 2005; Matsuo et al., 2005), and the highest expression of GPR139 receptors has been reported in the habenula (Matsuo et al., 2005; Wang et al., 2015; Hitchcock et al., 2016), a brain region that has been shown to be critically involved in addiction, anxiety, and mood regulation (Fowler and Kenny, 2012; Batalla et al., 2017). The role of orphan G protein–coupled receptors, including GPR139, in the pathophysiology of different diseases and disorders including anxiety, depression, schizophrenia, epilepsy, Alzheimer disease, Parkinson disease, and substance abuse disorders was recently discussed (Alavi et al., 2018).

Pharmacokinetics and biotransformation data from single oral in vivo administration of TAK-041 to rat, dog, monkey, and human suggest that TAK-041 not only is a slowly and extensively metabolized compound but also undergoes unusual multistep and sequential downstream metabolism. In addition, a notable species difference in the rate and the extent of metabolic pathways of TAK-041 was observed, with dogs having the highest metabolic clearance and humans the slowest. The terminal half-life ($t_{1/2}$) was ~3 hours in dog and ~11 days in human. To better understand the pharmacokinetic differences between species and

This paper received no external funding.
https://doi.org/10.1124/dmd.120.000246.

ABBREVIATIONS: ACN, acetonitrile; amu, atomic mass unit; CID, collision-induced dissociation; GPR139, G protein–coupled receptor 139; GSH, glutathione; HPLC, high-pressure liquid chromatography; LC/MS/MS, liquid chromatography with tandem mass spectrometry; MPCC, micropatterned coculture; *m/z*, mass-to-charge ratio; $t_{1/2}$, terminal half-life; TAK-041, (*S*)-2-(4-oxobenzo[d][1,2,3]triazin-3(4H)-yl)-*N*-(1-(4-(trifluoromethoxy)phenyl)ethyl)acetamide.

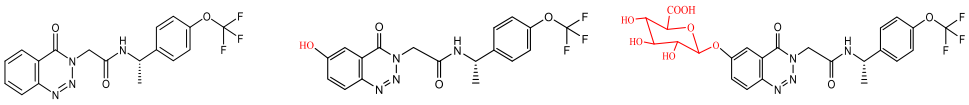

Fig. 1. Structures of TAK-041 and two of its metabolites, M2 and M4.

assess the biotransformation pathways in vitro, the metabolism of TAK-041 was initially studied using cryopreserved hepatocytes from rat, dog, monkey, and human. Because of the known limitations of cryopreserved suspended hepatocytes in maintaining drug-metabolizing enzyme activities for extended periods and in the expression of drug transporters (Gómez-Lechón et al., 2008, Ramsden et al., 2014), such conventional in vitro systems may not be well suited for evaluating slowly metabolized drug candidates such as TAK-041, adequately reflecting in vivo metabolites, or robustly characterizing metabolic pathways.

HepatoPac is a micropatterned coculture of rat, dog, monkey, and human hepatocytes that has been shown to address the challenge of predicting in vivo hepatic clearance of slowly metabolized compounds (Chan et al., 2019), enable long-term hepatic metabolism studies (Hutzler et al., 2015; Ballard et al., 2016; Chan et al., 2020), and evaluate the in vitro to in vivo extrapolation (Docci et al., 2020). The primary aim of this work was to evaluate the HepatoPac model as a suitable in vitro model to assess the biotransformation of slowly cleared GPR139 agonist TAK-041, determine any notable species difference in the rate and in the extent of its metabolic pathways, and attempt to establish a correlation between in vitro HepatoPac metabolites and in vivo metabolism.

TAK-041 was incubated for up to 14 days in rat, dog, monkey, and human HepatoPac models, and metabolic profiles were compared with their corresponding 2-hour incubation using conventional cryopreserved suspended hepatocytes. Findings from these studies and correlation with in vivo metabolic profiles from preclinical and clinical studies are reported herein.

Materials and Methods

Materials or General Chemicals. Commercially obtained chemicals and solvents were of high-performance liquid chromatography (HPLC) or analytical grade. Kinetex HPLC columns were obtained from Phenomenex (Torrance, CA). Cryopreserved suspended hepatocytes (rat, dog, monkey, and human) were obtained from Life Technologies (Grand Island, NY). HepatoPac cells (rat, dog, monkey, and human), reagents, and media components were provided by Hepregen Corp. (Medford, MA). Cells were plated in 24-well plates at the supplier's facility (Hepregen Corp.) and shipped overnight to Takeda, California. DMSO was purchased from Fisher Bioreagents (Pittsburg, PA).

Test Article and Reference Compounds. Test article TAK-041 and reference compounds metabolite M2 and metabolite M4 were synthesized at Takeda (San Diego, CA) and are shown in Fig. 1.

Cryopreserved Suspended Hepatocyte Incubation. A 2-μl aliquot of a 10 μM stock solution of TAK-041 in DMSO was added to 998 μl of Krebs-Henseleit buffer (pH 7.4) to prepare a 20 μM working solution for the hepatocyte incubation. The hepatocyte incubations consisted of (final concentrations) 10 μM TAK-041; approximately 100,000 cells per well of hepatocytes; cynomolgus monkey, lot CY359, one male donor; beagle dog, lot DB295, one male donor; Sprague-Dawley rat, lot RS688, three male donors; 0.1% DMSO; and Krebs-Henseleit at pH 7.4 made up to a final volume of 100 μl. Hepatocytes were thawed, processed, and prepared according to the protocol provided by the vendor to a working concentration of 2×10^6 cells per milliliter. A 96-well plate was used for this study. The hepatocyte suspension incubations were initiated with the addition of an equal volume of TAK-041 in incubation buffer to hepatocytes in the plate (final cell concentration of 1×10^6 cells per milliliter, 100-μl total well volume). Plates were incubated at 37°C for 0 and 2 hours, and the incubations were terminated by adding an equal volume of ice-cold acetonitrile (ACN). Precipitated protein was removed by centrifugation (6000 rpm for 10 minutes at room temperature), and the supernatant was analyzed by LC/MS/MS as described below.

HepatoPac Incubation. Upon receipt of HepatoPac cells and media components, two maintenance media were prepared and warmed to 37°C. One medium was for use with the rat wells and associated stromal and blank wells (rat media), and the other medium was for use with the dog, monkey, and human wells and associated stromal and blank wells (multispecies media). Supporting components were added to the base media per the recipe outlined and provided by the vendor. After preparation of maintenance media, HepatoPac cells preplated to 24-well plates were unpacked, and a full medium change was performed with the species-specific maintenance medium. Rat wells and associated stromal and blank wells were filled with 300 μl of maintenance media, and multispecies wells and associated stromal and blank wells were filled with 400 μl of maintenance media. Plates were incubated at 37°C in a 10% CO_2 atmosphere with >95% humidity for 48 hours. After incubation, two application media were prepared and warmed to 37°C. Supporting components were added to the base media per the recipe outlined and provided by the vendor.

TAK-041 (2.00 mg) was dispensed into a 4-ml glass vial and stored frozen at −20°C until use. DMSO (509.8 μl) was added to the vial to generate a 10 mM stock solution. An 80-μl aliquot of the 10 mM stock solution was added to 40 ml each of the prewarmed rat and multispecies application media inside a 50-ml conical tube to generate a 20 μM dosing solution. The fortified media were capped and stored at 37°C in a water bath until use.

Dosing. All plates were withdrawn from the maintenance media and replaced with their species-specific application media. The application media were withdrawn a second time and replaced with species-specific application media (300 μl for rat HepatoPac, stromal, and blank wells and 400 μl for multispecies HepatoPac, stromal, and blank wells). Cells were stored in the incubator until dosing. When ready for dosing, media in all wells were removed and replaced with fresh application media at half the final dosing volume (150 μl for rat, stromal, and blank wells and 200 μl for multispecies, stromal, and blank wells). An equal volume of species-specific 2× dosing solution was applied to each well and gently swirled.

Sample Collection. Samples were collected at 0, 2, 4, 24, 48, 168, and 336 hours postdose from multispecies wells and associated stromal and blank wells; a single well was used for each time point. For the 0-, 2-, and 4-hour time point samples, the blank application media were already prewarmed; for the 24-, 48-, 168-, and 336-hour time point samples, the blank application media were prewarmed to 37°C for 30 minutes prior to sampling. At each time point, 250 μl (rat wells) and 350 μl (multispecies wells) of media were removed from the HepatoPac, stromal, and blank wells and quenched with 500 μl (rat wells) or 700 μl (multispecies wells) of ice-cold ACN in polypropylene tubes; these were referred to as the primary samples. A 250-μl (rat wells) or 350-μl (multispecies wells) aliquot of blank application media were added back to each well, and all contents were removed and quenched with 600 μl (rat wells) or 800 μl (multispecies wells) of ice-cold ACN in polypropylene tubes; these were referred to as the wash samples. Ice-cold ACN (600 μl for rat wells and 800 μl for multispecies wells) was added back to the wells. Using the edge of a 1000-μl pipette tip, the well was scraped thoroughly from side to side starting at the top and moving to the bottom. After thorough scraping, all ACN was removed and transferred to polypropylene tubes; these were referred to as the cell lysate samples. After all samples were collected, an aliquot of 300 μl (rat wells) or 400 μl (multispecies wells) of application media were returned to the wells to maintain the local humidity for the remaining samples.

Sample Processing. Cell lysate samples were stored frozen at −80°C without immediate processing for future analysis. Primary and wash samples were gently rotated manually several times to ensure thorough mixing of sample and quench solutions and then centrifuged at 3000 rpm for 30 minutes on an Allegra X-14R centrifuge (Beckman Coulter, Brea, CA). Supernatant (500 μl for rat samples and 800 μl for multispecies samples) was collected and transferred to fresh

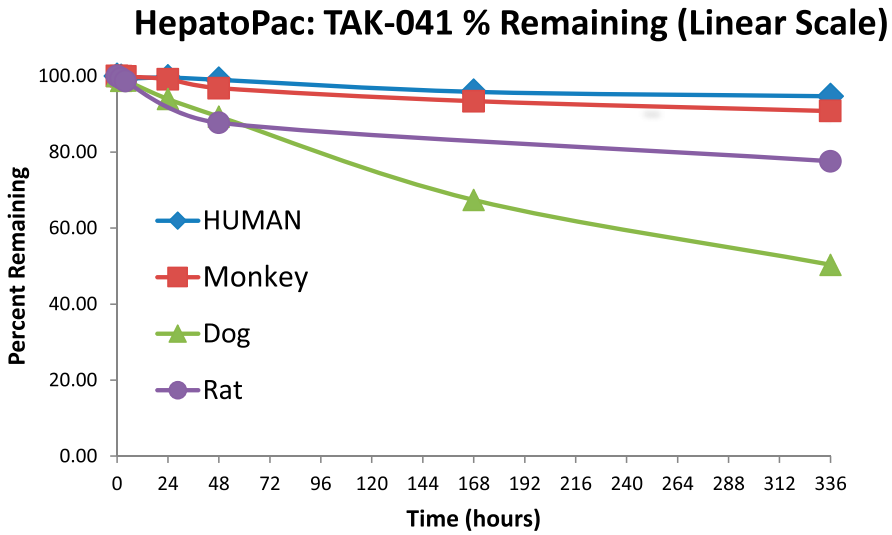

Percentage of Total Peak Area of TAK-041 remaining from Day 14 HepatoPac Incubation

Metabolite	Biotransformation	Human	Monkey	Dog	Rat
TAK-041	Parent	94.2	90.7	47.7	76.7

Fig. 2. Total peak area-time profiles of TAK-041% remaining (linear and log scale) after HepatoPac incubation for up to 14 days in rat, dog, monkey, and human.

polypropylene tubes and stored frozen at −80°C until analysis. Tubes containing residual quench solution and protein pellet were stored frozen at −80°C for possible future analysis. Immediately preceding liquid chromatography–mass spectrometry analysis, the supernatants from the primary and wash samples were combined and dried under nitrogen. Samples were reconstituted in water containing 5% ACN and analyzed by liquid chromatography–mass spectrometry as described below.

In Vivo Circulating Metabolites. Plasma samples from a single oral administration of TAK-041 to rat (5 mg/kg), dog (10 mg/kg), monkey (15 mg/kg), and human (5 mg, subjects 1201, 1203, 1204, 1206, 1207, and 1208) were pooled for metabolite profiling and identification. Plasma samples were pooled using Hamilton's method (Hamilton et al., 1981) using the area under the plasma concentration-time curve from time 0 to 24 hours (rat and dog) and from 0 to 96 hours (monkey and human). Proteins were precipitated with three volumes of acetonitrile and mixed thoroughly. The sample was centrifuged, and supernatant was removed. The pellet was resuspended with 2 ml of 80:20 ACN/water, mixed, and centrifuged. Supernatants were combined, dried under nitrogen, and reconstituted with 80:20 water/ACN (0.1% formic acid) for analysis by LC/MS/MS as described below.

Liquid Chromatography and Tandem Mass Spectrometry Analysis. Aliquots of the supernatants were injected onto an LC/MS/MS system consisting of a Shimadzu LC-20AD (Shimadzu Scientific Instruments Corp., Columbia, MD) HPLC system with a Kinetex 5-μm C18 column (2.1 × 150 mm; Phenomenex, Inc.). Chromatographic separations were performed under ambient conditions using a gradient elution with solvent A (0.1% formic acid in water) and solvent B (0.1% formic acid in acetonitrile). The gradient was initiated at a 95:5 A/B ratio at a flow rate of 0.4 ml/min and held for 4 minutes, ramped linearly from 5% B to 40% B over 14 minutes, to 60% B over the next 4 minutes, and then to 90% B over 2 minutes and held for 2 minutes. The column re-equilibration time was 7 minutes (total run time of 35 minutes). The HPLC eluent was introduced into an AB Sciex TripleTOF 5600 mass spectrometer (Applied Biosystems, Inc., Foster City, CA) operated in positive ion mode at an ion source voltage floating of 5 kV. The source temperature was set at 500°C with source gas 1 and source gas 2 both set to 60 U and curtain gas set to 25 U. The mass range of full-scan mass spectrometry was 100–1300 Da. The tandem mass spectrometry spectra for information-dependent acquisition were obtained using a collision energy of 45.

Results

Incubation of TAK-041 in a suspension of cryopreserved hepatocytes (rat, dog, monkey, and human) for 2 hours to estimate and compare major metabolites in human and preclinical species resulted in no metabolic turnover in human, and minimal metabolic turnover was observed in rat, dog, and monkey. In contrast, after incubation in the HepatoPac hepatocyte coculture model for up to 14 days, more metabolic turnover and robust metabolite generation were observed, as evident by the percentage of TAK-041 remaining and the total number of metabolites detected. Although 0-, 2-, 4-, 24-, 48-, 168-, and 336-hour time points were collected for TAK-041, day 14 (336 hours) was selected to illustrate appreciable and downstream metabolism. Some early time points (2, 4, 24, and 48 hours) were also selected to assess upstream metabolism including the formation of the glutathione conjugate of TAK-041. The percentage of peak area of 10 μM TAK-041 after 14-day incubation was ~77%, 48%, 91%, and 94% in rat, dog, monkey, and human, respectively, suggesting a faster rate of metabolism in dog compared with other species (Fig. 2). These in vitro findings are consistent with the mean plasma concentration-time profiles of TAK-041 in rat, dog, monkey, and human after single-dose oral administration, as graphically depicted in Fig. 3, showing dogs with much less prolonged terminal half-life and faster clearance rate compared with other species, with dogs having the highest metabolic clearance and humans the slowest. The $t_{1/2}$ was ~3 hours in dog and ~11 days in human (unpublished data).

Comparison of In Vitro Metabolites of TAK-041 in Cryopreserved Suspended Hepatocytes and HepatoPac Model with In Vivo Circulating Metabolites. Incubation of TAK-041 in a suspension of cryopreserved hepatocytes produced three metabolites in rat (M2, M4/M12), five metabolites in dog (M1, M2, M4/M12, M11), four metabolites in monkey (M1, M2, M4/M12), and no metabolites in human. In contrast, more metabolic turnover and robust metabolite

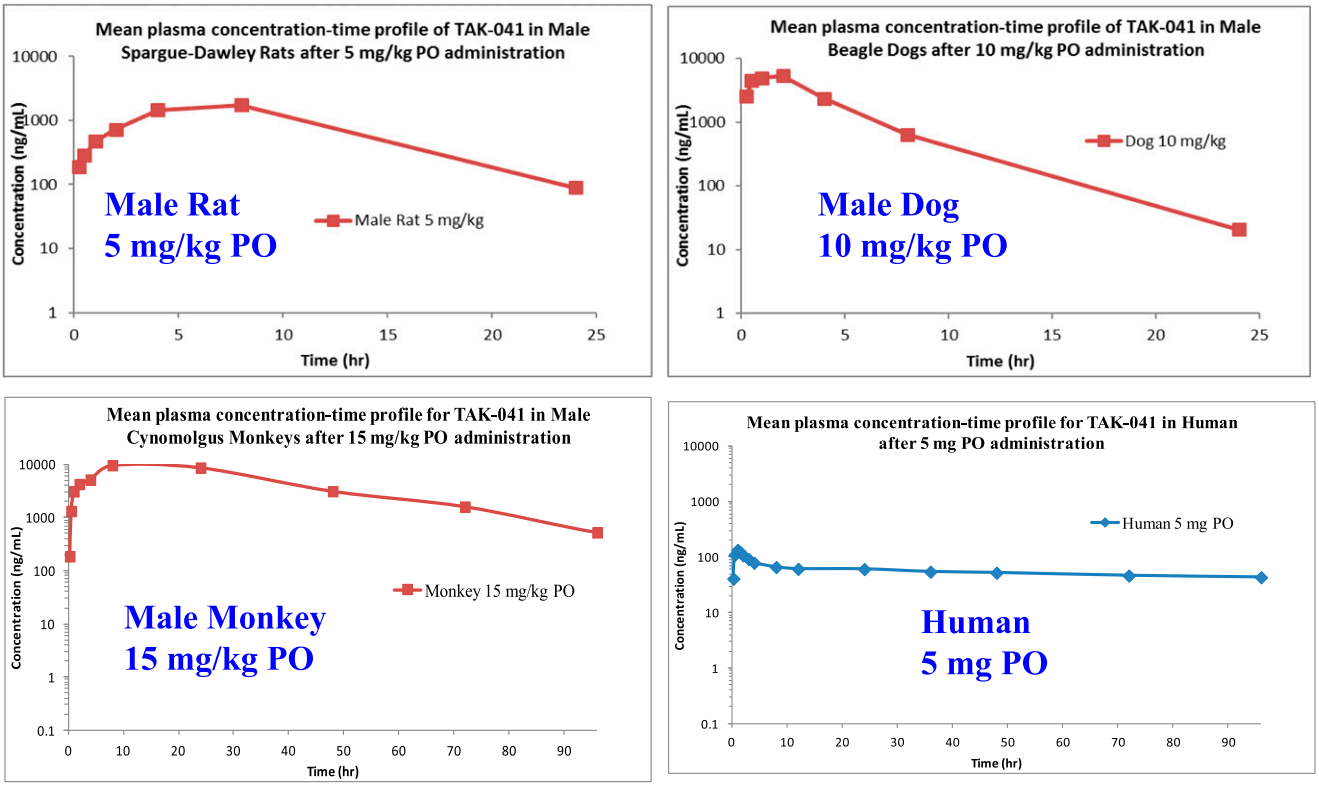

Fig. 3. Comparison of mean plasma concentration-time profiles for TAK-041 in rat, dog, monkey, and human after single-dose oral administration. PO, per os.

generation were observed in the HepatoPac model, which produced 10 metabolites in rat (M1, M2, M3, M4/M12, M5, M6, M7, M8, and M10), 9 metabolites in dog (M1, M2, M3, M4/M12, M6, M7, M8, and M10), 7 metabolites in monkey [M1, M2, M3, M4/M12, M5, M6, M7 (trace level), M8, and M10], and 9 metabolites in human (M1, M2, M3, M4/M12, M5, M7, M8, and M9). It is worth pointing out that M9 is not unique to human, although it was only observed in human HepatoPac. This could be explained by the fact the formation of M9 (methylsulfoxide of TAK-041) is a prerequisite for the formation of M7 (methylsulfone of TAK-041), which was observed in all species. Rat, dog, monkey, and human in vivo circulating metabolites were all observed at an appreciable level with their corresponding HepatoPac model. A summary of in vitro metabolites after incubation in hepatocyte suspension and HepatoPac model and comparison with in vivo circulating metabolites in rat, dog, monkey, and human are presented in Tables 1–4, respectively.

In addition to plasma metabolites, it is noteworthy to point out that urinary, fecal, and biliary metabolites from preclinical species and humans, when applicable, were compared with in vitro metabolites. The most abundant urinary metabolite in preclinical and humans was M2, whereas M1, M3, and M4 were also detected at much lower levels. M4 was the major drug-related metabolite in feces of preclinical species, with TAK-041, M1, M6, M7, M10, and M11 detected at small amounts. In bile duct cannulated rats, M2 and M11 were the predominant metabolites in bile, whereas M1 was less prominent (unpublished data).

TABLE 1

Summary of metabolites after incubation in rat hepatocyte suspension (2 h) and HepatoPac model (14 day) and comparison with in vivo circulating metabolite

Metabolite	Biotransformation Reaction	$[M + H]^+$ (Calculated)	Rat Hepatocyte Suspension	Rat HepatoPac Model	In Vivo Rat Circulating Metabolite
TAK-041	Parent drug	393.1169	Observed	Observed	Observed
M1	Cysteine conjugation	512.121	—	Observed	—
M2	Hydroxylation and glucuronide conjugation	585.1439	Observed	Observed	Observed
M3	*N*-acetylcysteine conjugation	554.1316	—	Observed	—
M4/M12[a]	Hydroxylation	409.1118	Observed	Observed	Observed
M5	Oxidative *N*-dealkylation and reduction	264.0842	—	Observed	—
M6	Hydroxylation	409.1118	—	Observed	—
M7	Methylsulfone conjugation	471.0945	—	Observed	Observed
M8	Methylsulfide conjugation	439.1046	—	Observed	—
M9	Methylsulfoxide conjugation	455.0995	—	—	Observed
M10	Hydroxylation and sulfate conjugation	489.0686	—	Observed	—
M11[b]	Glutathione conjugation	698.1851	—	—	—
M13	Ring closure and hydrolysis	274.0798	—	Trace level	—

—, not detected.
[a]Metabolites M4 and M12 represent isomeric structures.
[b]M11 was detected at trace level from 24- and 48-h incubations.

TABLE 2

Summary of metabolites after incubation in dog hepatocyte suspension (2 h) and HepatoPac model (14 day) and comparison with in vivo circulating metabolite

Metabolite	Biotransformation Reaction	$[M + H]^+$ (Calculated)	Dog Hepatocyte Suspension	Dog HepatoPac Model	In Vivo Dog Circulating Metabolite
TAK-041	Parent drug	393.1169	Observed	Observed	Observed
M1	Cysteine conjugation	512.121	Observed	Observed	Observed
M2	Hydroxylation and glucuronide conjugation	585.1439	Observed	Observed	Observed
M3	*N*-acetylcysteine conjugation	554.1316	—	Observed	—
M4/M12[a]	Hydroxylation	409.1118	Observed	Observed	Observed
M5	Oxidative *N*-dealkylation and reduction	264.0842	—	—	Observed
M6	Hydroxylation	409.1118	—	Observed	Observed
M7	Methylsulfone conjugation	471.0945	—	Observed	Observed
M8	Methylsulfide conjugation	439.1046	—	Observed	Observed
M9	Methylsulfoxide conjugation	455.0995	—	—	—
M10	Hydroxylation and sulfate conjugation	489.0686	—	Observed	—
M11[b]	Glutathione conjugation	698.1851	Observed	—	—
M13	Ring closure and hydrolysis	274.0798	—	Trace level	Observed

—, not detected.
[a]Metabolites M4 and M12 represent isomeric structures.
[b]M11 was detected at trace level from 2-, 4-, 24-, 48-, and 168-h incubations.

Identification of Metabolites. The structures of metabolites were elucidated by ion spray LC/MS/MS and based on accurate mass measurements and elemental composition. When possible, the identities of metabolites were confirmed by coelution on HPLC with synthetic standards. The word "tentative" was used when synthetic standards were unavailable and/or the exact sites of some structural modification could not be determined.

Synthetic standard of TAK-041 had a retention time of ~21.5 minutes on the HPLC system and showed a protonated molecular ion at mass-to-charge ratio (*m/z*) 393.1173. The collision-induced dissociation (CID) mass spectrum of TAK-041 and proposed structures for characteristic fragments ions are shown in Fig. 4. The CID mass spectrum of TAK-041 showed fragment ions at *m/z* 177.0660, 149.0704, and 132.0443, which are derived from the oxobenzotriazine acetamide moiety. The fragment ion at *m/z* 190.0561 represented the oxobenzotriazine acetaldehyde moiety. The fragment ion at *m/z* 189.0522 was the most abundant ion in TAK-041 mass spectrum and represented the trifluoromethoxy phenyl ethyl moiety. The fragment ion at *m/z* 103.0540 was derived from the fragment ion at *m/z* 189.0521 via the loss of trifluoromethanol molecule.

TAK-041 and a total of 13 metabolites were identified, and unchanged drug was the major circulating metabolite in all species and most abundant in all in vitro incubations across species.

M1. M1 had a retention time of ~17.1 minutes on the HPLC system and showed a protonated molecular ion at *m/z* 512.1221, 119.0048 mass units higher than that of the unchanged drug (*m/z* 393.1173), suggesting it was a conjugate. Its CID spectrum is depicted in Fig. 5 and showed the fragment ions at *m/z* 189.0524 and 103.0534, indicating that the modification had occurred remote from the trifluoromethoxy phenyl ethyl moiety. The fragment ions at *m/z* 296.0691 and 251.0482, 119.0048 Da higher than the fragment ions at *m/z* 177.0660 and 132.0443 of the unchanged drug, further suggested that M1 was a conjugate and the oxobenzotriazine acetamide moiety was the site of modification. The fragment ion at *m/z* 279.0459 (loss of ammonia, 17.0232 atomic mass unit (amu), from the fragment ion at *m/z* 296.0691) further suggested that the modification had occurred on the oxobenzotriazine moiety and likely on the phenyl ring. The fragment ion at *m/z* 222.0223, 31.9662 mass units higher than the fragment ion at *m/z* 190.0561 of the unchanged drug, suggested an incorporation of a sulfur atom most likely on the phenyl ring. The loss of 87.0320 mass units (aminoacrylic acid) from the conjugate and incorporation of the sulfur atom further suggested that M1 was a cysteine conjugate. The exact position of the cysteine addition could not be determined from mass spectral data. Based on these data, M1 was tentatively identified as the cysteine conjugate of TAK-041.

M2. M2 had a retention time of ~17.4 minutes on the HPLC system and showed a protonated molecular ion at *m/z* 585.1456, 192.0283 mass units higher than that of the unchanged drug (*m/z* 393.1173), suggesting it was a conjugate. The fragment ion at *m/z* 369.0944, 192.0280 Da

TABLE 3

Summary of metabolites after incubation in monkey hepatocyte suspension (2 h) and HepatoPac model (14 day) and comparison with in vivo circulating metabolite

Metabolite	Biotransformation Reaction	$[M + H]^+$ (Calculated)	Monkey Hepatocyte Suspension	Monkey HepatoPac Model	In Vivo Monkey Circulating Metabolite
TAK-041	Parent drug	393.1169	Observed	Observed	Observed
M1	Cysteine conjugation	512.121	Observed	Observed	—
M2	Hydroxylation and glucuronide conjugation	585.1439	Observed	Observed	Observed
M3	*N*-acetylcysteine conjugation	554.1316	—	—	—
M4/M12[a]	Hydroxylation	409.1118	Observed	Observed	Observed
M5	Oxidative *N*-dealkylation and reduction	264.0842	—	—	—
M6	Hydroxylation	409.1118	—	Observed	—
M7	Methylsulfone conjugation	471.0945	—	Trace level	Observed
M8	Methylsulfide conjugation	439.1046	—	—	Observed
M9	Methylsulfoxide conjugation	455.0995	—	—	—
M10	Hydroxylation and sulfate conjugation	489.0686	—	Observed	—
M11[b]	Glutathione conjugation	698.1851	—	—	—
M13	Ring closure and hydrolysis	274.0798	—	Trace level	—

—, not detected.
[a]Metabolites M4 and M12 represent isomeric structures.
[b]M11 was detected at trace level from 24- and 48-h incubations.

TABLE 4

Summary of metabolites after incubation in human hepatocyte suspension (2 h) and HepatoPac model (14 day) and comparison with in vivo circulating metabolite

Metabolite	Biotransformation Reaction	$[M + H]^+$ (Calculated)	Human Hepatocyte Suspension	Human HepatoPac Model	In Vivo Human Circulating Metabolite
TAK-041	Parent drug	393.1169	Observed	Observed	Observed
M1	Cysteine conjugation	512.121	—	Observed	Observed
M2	Hydroxylation and glucuronide conjugation	585.1439	—	Observed	Observed
M3	*N*-acetylcysteine conjugation	554.1316	—	Observed	Observed
M4/M12[a]	Hydroxylation	409.1118	—	Observed	Observed
M5	Oxidative *N*-dealkylation and reduction	264.0842	—	Observed	—
M6	Hydroxylation	409.1118	—	—	—
M7	Methylsulfone conjugation	471.0945	—	Observed	Trace level
M8	Methylsulfide conjugation	439.1046	—	Observed	Trace level
M9	Methylsulfoxide conjugation	455.0995	—	Observed	Trace level
M10	Hydroxylation and sulfate conjugation	489.0686	—	—	—
M11	Glutathione conjugation	698.1851	—	—	—
M13	Ring closure and hydrolysis	274.0798	—	Trace level	—

—, not detected.
[a]Metabolites M4 and M12 represent isomeric structures.

higher than the fragment ion at *m/z* 177.0660 of the unchanged drug, further suggested that M2 was a conjugate. Its CID spectrum is depicted in Fig. 6 and showed the fragment ions at *m/z* 409.1130, a loss of 176.0326 mass units, suggesting M2 was a glucuronide conjugate. The fragment ion at *m/z* 409.1130, 15.9957 mass units higher than the molecular ion of unchanged drug, suggested the addition of an oxygen atom to the molecule. Further collision-induced dissociation of the fragment ion at *m/z* 409.1130 showed the fragment ions at *m/z* 189.0523 and 103.0542, indicating that the hydroxylation had occurred remote from the trifluoromethoxy phenyl ethyl moiety. The fragment ions at *m/z* 193.0611, 165.0657, and 148.0395 (15.9951, 15.9953, and 15.9952 Da higher than the fragment ions at *m/z* 177.0660, 149.0704, and 132.0443 of the unchanged drug, respectively) further suggested that the oxobenzotriazine acetamide moiety was the site of hydroxylation. The absence of water loss (18.0106 amu) in the CID spectrum of M2 suggested that aliphatic hydroxylation had not occurred and that the hydroxylation has occurred at the phenyl ring fused to the oxotriazine moiety. M2 coeluted with the synthetic standard on HPLC, and its CID spectrum was identical. Based on these data, M2 was identified as the 6-*O*-glucuronide conjugate of TAK-041 (the glucuronide conjugate of M4).

M3. M3 had a retention time of ~19.2 minutes on the HPLC system and showed a protonated molecular ion at *m/z* 554.1302, 161.0129 mass units higher than that of the unchanged drug (*m/z* 393.1173), suggesting it was a conjugate. Its CID spectrum (data not shown) showed the fragment ion at *m/z* 189.0517, indicating that the modification had occurred remote from the trifluoromethoxy phenyl ethyl moiety. The fragment ion at *m/z* 338.0800, 161.0140 Da higher than the fragment ions at *m/z* 177.0660 of the unchanged drug, further suggested that M3 was a conjugate and that the oxobenzotriazine acetamide moiety was the site of modification. The fragment ion at *m/z* 321.0405 (loss of ammonia, 17.0232 amu, from the fragment ion at *m/z* 338.0800) further suggested that the modification had occurred on the oxobenzotriazine moiety and likely on the phenyl ring. Based on these data, M3 was tentatively identified as the acetyl conjugate of M1.

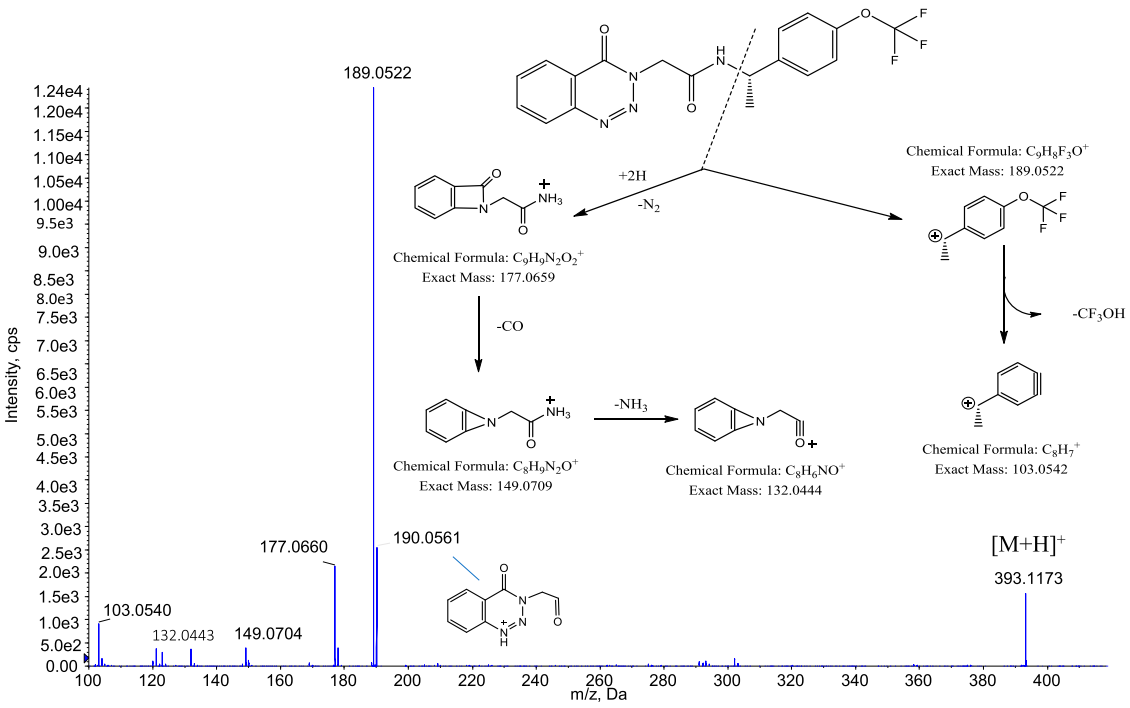

Fig. 4. CID mass spectrum of synthetic standard of TAK-041 at *m/z* 393 and proposed structures for characteristic fragment ions. cps, counts per second.

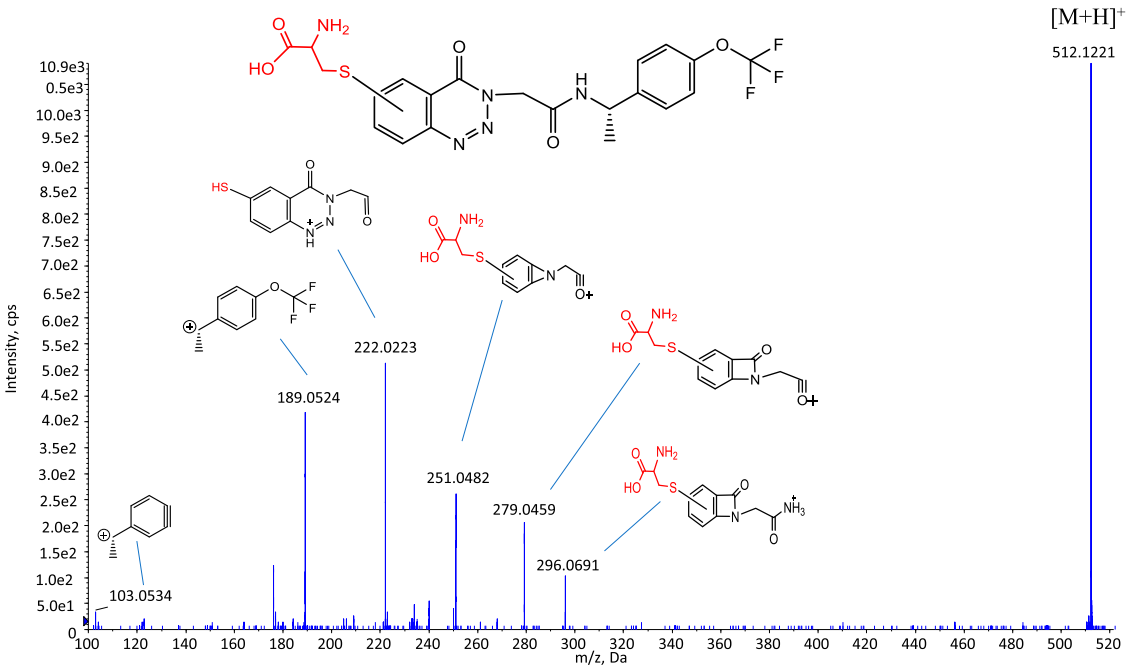

Fig. 5. CID mass spectrum of M1 at *m/z* 512. cps, counts per second.

M4. M4 had a retention time of ~20.5 minutes on the HPLC system and showed a protonated molecular ion of *m/z* 409.1140, 15.9967 mass units higher than that of the unchanged drug (*m/z* 393.1173), suggesting that the molecule had undergone mono-oxidation. Its CID spectrum is depicted in Fig. 7 and showed the fragment ions at *m/z* 189.0526 and 103.0543, indicating that the hydroxylation had occurred remote from the trifluoromethoxy phenyl ethyl moiety. The fragment ions at *m/z* 193.0616, 165.0660, and 148.0394 (15.9956, 15.9956, and 15.9951 Da higher than the fragment ions at *m/z* 177.0660, 149.0704, and 132.0443 of the unchanged drug, respectively) further suggested that the oxobenzotriazine acetamide moiety was the site of hydroxylation. The absence of water loss (18.0106 amu) in the CID spectrum of M4 suggested that aliphatic hydroxylation had not occurred and that the hydroxylation has occurred at the phenyl ring fused to the oxotriazine moiety. M4 coeluted with the synthetic standard and its CID spectrum was identical. Based on these data, M4 was identified as the 6-OH metabolite of TAK-041.

M5. M5 had a retention time of ~16.4 minutes on the HPLC system and showed a protonated molecular ion at *m/z* 264.0845, 129.0328 mass units lower than that of the unchanged drug (*m/z* 393.1173), suggesting

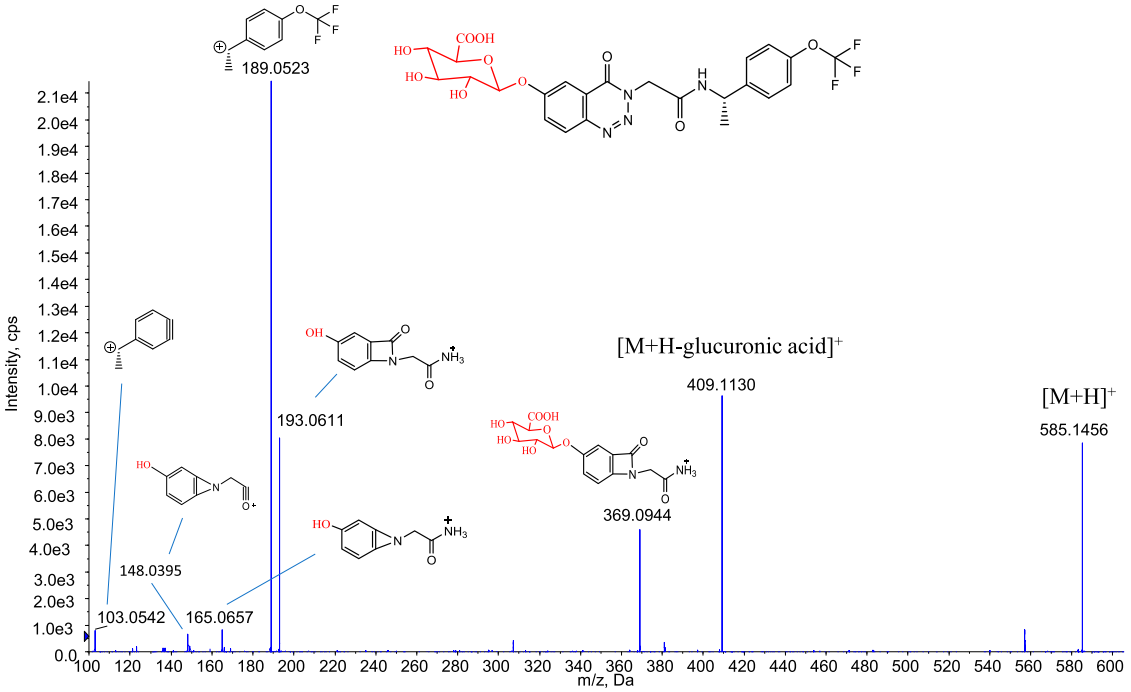

Fig. 6. CID mass spectrum of M2 at *m/z* 585. cps, counts per second.

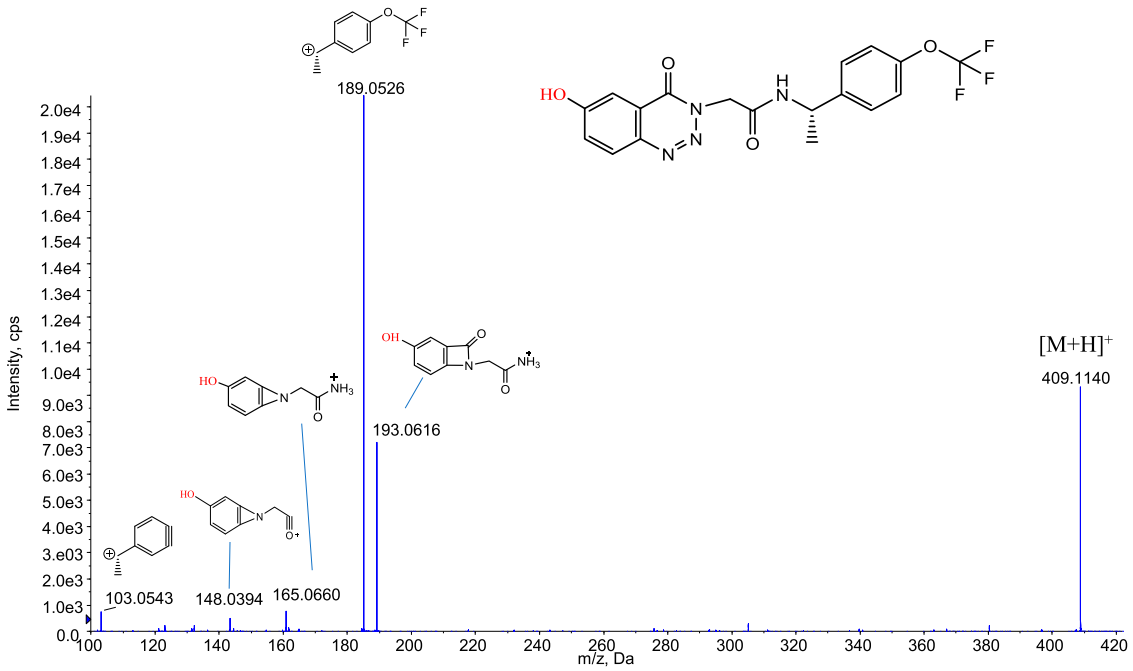

Fig. 7. CID mass spectrum of M4 at *m/z* 409. cps, counts per second.

that M5 was a cleaved product. Its CID spectrum (data not shown) showed the fragment ions at *m/z* 189.0524 (the most abundant ion) and 103.0539, indicating that the trifluoromethoxy phenyl ethyl moiety was intact. Oxidation at the carbon α to *N*-3 of the triazine-4-one moiety to form unstable carbinolamine followed by release of oxobenzotriazine moiety and subsequent reduction to the corresponding alcohol leads to the formation of M5. Based on these data, M5 was tentatively identified as 2-hydroxy-*N*-(4-(trifluoromethoxy)benzyl)acetamide.

M6. M6 had a retention time of ~18.4 minutes on the HPLC system and also showed a protonated molecular ion at *m/z* 409.1125, 15.9952 mass units higher than that of the unchanged drug (*m/z* 393.1173), suggesting that the molecule had undergone mono-oxidation. Its CID spectrum (data not shown) showed the fragment ion at *m/z* 177.0654, indicating that the hydroxylation had occurred remote from the oxobenzotriazine acetamide moiety. The fragment ions at *m/z* 119.0475 and 205.0505, 15.9935 and 15.9983 Da higher than the fragment ions at *m/z* 103.0540 and 189.0522 of the unchanged drug, respectively, further suggested that the trifluoromethoxy phenyl ethyl moiety was the site of hydroxylation. The absence of water loss (18.0106 amu) in the CID spectrum of M6 suggested that aliphatic hydroxylation had not occurred and that the hydroxylation has occurred at the phenyl ring. The exact position of the hydroxylation could not be determined from mass spectral data. Based on these data, M6 was tentatively identified as the hydroxyl metabolite of TAK-041.

M7. M7 had a retention time of ~20.6 minutes on the HPLC system and showed a protonated molecular ion at *m/z* 471.0968, 77.9795 mass units higher than that of the unchanged drug (*m/z* 393.1173). Its CID spectrum is depicted in Fig. 8 and showed the fragment ions at *m/z* 189.0525 and 103.0541, indicating that the modification had occurred remote from the trifluoromethoxy phenyl ethyl moiety. The fragment ions at *m/z* 255.0441, 227.0492, and 210.0221 (77.9781, 77.9788, and 77.9778 Da higher than the fragment ions at *m/z* 177.0660, 149.0704, and 132.0443, respectively, of the unchanged drug) suggested that the oxobenzotriazine moiety was the site of modification. The fragment ion at *m/z* 210.0221 (loss of ammonia, 17.0271 amu, from the fragment ion at *m/z* 227.0492) further suggested that the modification had occurred on oxobenzotriazine moiety and likely on the phenyl ring. Based on these data, M7 was tentatively identified as the methylsulfone of TAK-041 (oxidative product of M9).

M8. M8 had a retention time of ~22.5 minutes on the HPLC system and showed a protonated molecular ion at *m/z* 439.1048, 45.9875 mass units higher than that of the unchanged drug (*m/z* 393.1173). Its CID spectrum is depicted in Fig. 9 and showed the fragment ions at *m/z* 189.0519 and 103.0532, indicating that the modification had occurred remote from the trifluoromethoxy phenyl ethyl moiety. The fragment ions at *m/z* 223.0528, 195.0586, and 178.0319 (45.9868, 45.9882, and 45.9876 Da higher than the fragment ions at *m/z* 177.0660, 149.0704, and 132.0443, respectively, of the unchanged drug) suggested that the oxobenzotriazine moiety was the site of modification. The fragment ion at *m/z* 178.0319 (loss of ammonia, 17.0267 amu, from the fragment ion at *m/z* 195.0586) further suggested that the modification had occurred on oxobenzotriazine moiety and likely on the phenyl ring. Based on these data, M8 was tentatively identified as the methylsulfide of TAK-041.

M9. M9 had a retention time of ~19.1 minutes on the HPLC system and showed a protonated molecular ion at *m/z* 455.0995, 61.9822 mass units higher than that of the unchanged drug (*m/z* 393.1173). Its CID spectrum (data not shown) showed the fragment ions at *m/z* 189.0523 and 103.0542, indicating that the modification had occurred remote from the trifluoromethoxy phenyl ethyl moiety. The fragment ions at *m/z* 239.0489, 211.0534, and 194.0258 (61.9829, 61.9830, and 61.9815 Da higher than the fragment ions at *m/z* 177.0660, 149.0704, and 132.0443, respectively, of the unchanged drug) suggested that the oxobenzotriazine moiety was the site of modification. The fragment ion at *m/z* 194.0258 (loss of ammonia, 17.0276 amu, from the fragment ion at *m/z* 211.0534) further suggested that the modification had occurred on oxobenzotriazine moiety and likely on the phenyl ring. Based on these data, M9 was tentatively identified as the methylsulfoxide of TAK-041 (oxidative product of M8).

M10. M10 had a retention time of ~18.6 minutes on the HPLC system and showed a protonated molecular ion at *m/z* 489.0675, 95.9502 mass units higher than that of the unchanged drug (*m/z* 393.1173), suggesting it was a conjugate. The fragment ion at *m/z* 273.0126,

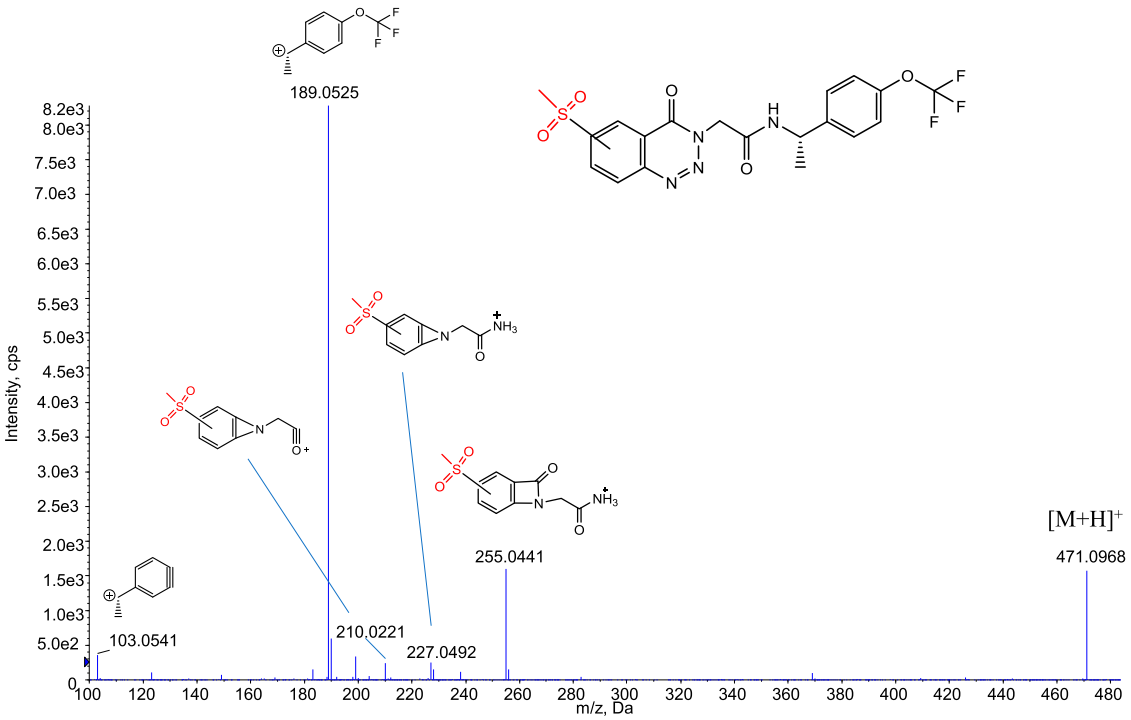

Fig. 8. CID mass spectrum of M7 at *m/z* 471. cps, counts per second.

95.9502 Da higher than the fragment ion at *m/z* 177.0660 of the unchanged drug, further suggested that M10 was a conjugate. Its CID spectrum (data not shown) showed the fragment ions at *m/z* 409.1128, a loss of 79.9547 mass units, suggesting M10 was a sulfate conjugate. The fragment ion at *m/z* 409.1128, 15.9955 mass units higher than the molecular ion of unchanged drug (*m/z* 393.1173), suggested the addition of an oxygen atom to the molecule. Further collision-induced dissociation of the fragment ion at *m/z* 409.1128 showed the fragment ions at *m/z* 189.0519 and 103.0531, indicating that the hydroxylation had occurred remote from the trifluoromethoxy phenyl ethyl moiety. The fragment ion at *m/z* 193.0623, 15.9963 Da higher than the fragment ions at *m/z* 177.0660 of the unchanged drug, further suggested that the oxobenzotriazine acetamide moiety was the site of hydroxylation. The absence of water loss (18.0106 amu) in the CID spectrum of M10 suggested that aliphatic hydroxylation had not occurred and that the hydroxylation has occurred on the phenyl ring fused to the oxotriazine moiety. The exact position of the hydroxylation could not be determined from mass spectral data. Based on these data, M10 was tentatively identified as the sulfate conjugate of the hydroxyl metabolite M4/M12.

M11. M11 had a retention time of ~16.5 minutes on the HPLC system and showed a protonated molecular ion at *m/z* 698.1848, 305.0675 mass units higher than that of the unchanged drug (*m/z*

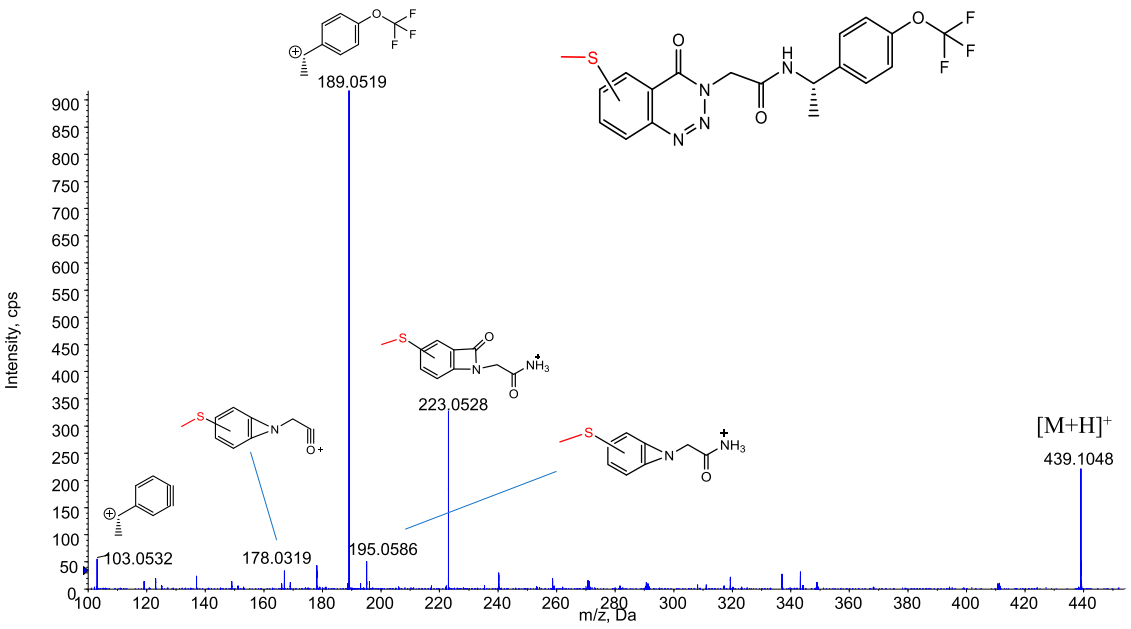

Fig. 9. CID mass spectrum of M8 at *m/z* 439. cps, counts per second.

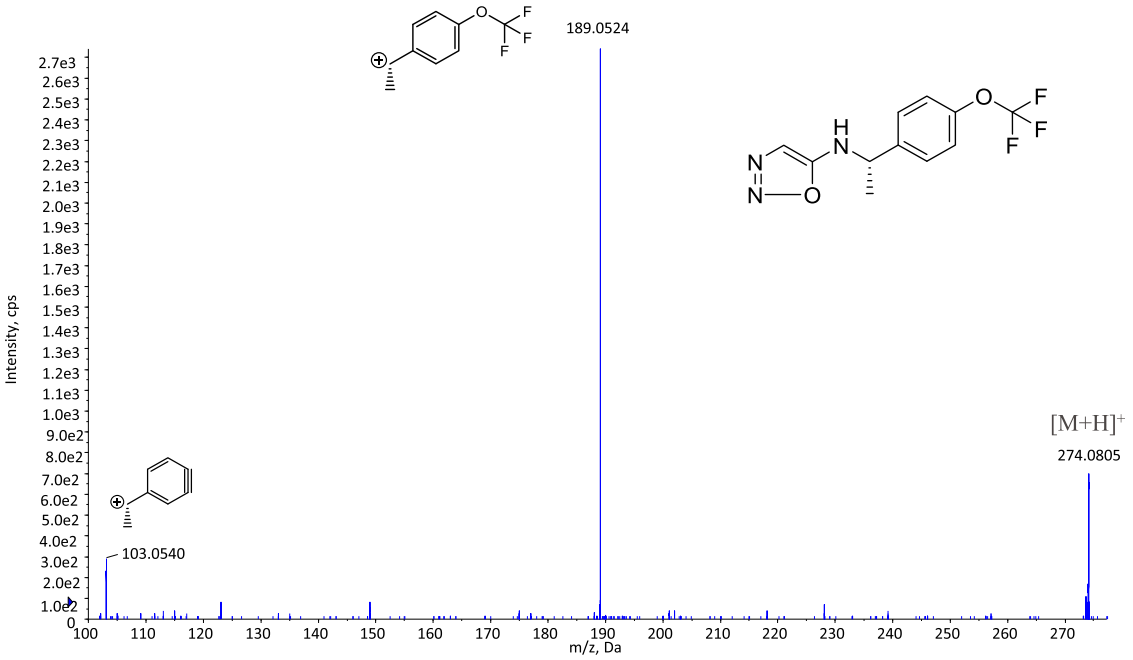

Fig. 10. CID mass spectrum of M13 at *m/z* 274. cps, counts per second.

393.1173), suggesting it was a conjugate. Its CID spectrum (data not shown) showed characteristic fragment ions at *m/z* 623.1523 and 569.1436 and loss of 75.0325 mass units (glycine molecule) and 129.0412 mass units (pyroglutamic acid), suggesting that M11 was a glutathione (GSH) conjugate. The fragment ion at *m/z* 189.0524 indicated that the glutathione addition had occurred remote from the trifluoromethoxy phenyl ethyl moiety and that the oxobenzotriazine acetamide moiety was the site of addition. The exact position of GSH addition could not be determined from mass spectral data. Based on these data, M11 was tentatively identified as the GSH conjugate of TAK-041.

M12. M12 had a retention time of ~20.2 minutes on the HPLC system and showed a protonated molecular ion of *m/z* 409.1108, 15.9935 mass units higher than that of the unchanged drug (*m/z* 393.1173), suggesting that the molecule had undergone mono-oxidation. Its CID spectrum (data not shown) showed the fragment ions at *m/z* 103.0590 and 189.0522, indicating that the hydroxylation had occurred remote from the trifluoromethoxy phenyl ethyl moiety. The fragment ions at *m/z* 193.0657, 165.0652, and 148.0400 (15.9997, 15.9948, and 15.9957 Da higher than the fragment ions at *m/z* 177.0660, 149.0704, and 132.0443 of the unchanged drug, respectively) further suggested that the oxobenzotriazine acetamide moiety was the site of hydroxylation. The absence of water loss (18.0106 amu) in the CID spectrum of M12 suggested that aliphatic hydroxylation had not occurred and that the hydroxylation has occurred on the phenyl ring fused to the oxotriazine moiety. The exact position of the hydroxylation could not be determined from mass spectral data. Based on these data, M12 was tentatively identified as the isomeric structure of M4.

M13. M13 had a retention time of ~19.2 minutes on the HPLC system and showed a protonated molecular ion at *m/z* 274.0805, 119.0368 mass units lower than that of the unchanged drug (*m/z* 393.1173), suggesting that M13 was a cleaved product with an odd number of nitrogen atoms. Its CID spectrum is depicted in Fig. 10 and showed the fragment ions at *m/z* 189.0524 (the most abundant ion) and 103.0540, indicating that the trifluoromethoxy phenyl ethyl moiety was intact. The fragment ion at *m/z* 189.0524, loss of 85.0281 mass units (oxadiazole amine), from the protonated molecular ion, further indicated that M13 contained three nitrogen atoms and that aminobenzaldehyde (loss of 119.0368 mass units) has been removed from the unchanged drug. The accuracy of both the theoretical mass of M13 (*m/z* 274.0798) and its empirical formula ($C_{11}H_{11}F_3N_3O_2$) was ≤ ± 2.5 ppm error and further suggested the proposed structure. Based on these data, M13 was tentatively identified as (*S*)-*N*-(1-(4-(trifluoromethoxy)phenyl)ethyl)-1,2,3-oxadiazol-5-amine.

Discussion

The metabolism of slowly cleared clinical candidate TAK-041 was studied in two different in vitro model systems using rat, dog, monkey, and human suspended cryopreserved hepatocytes and HepatoPac and compared with relevant metabolites reported in human and preclinical species in vivo studies.

TAK-041 was slowly yet extensively metabolized since only a small or no amount of unchanged drug was detected in the excreta (unpublished data). In addition to unchanged drug, a total of 13 metabolites are reported. TAK-041 undergoes both phase I and II metabolism. The major biotransformation pathways of TAK-041 proceed via hydroxylation on the benzene ring fused to the oxotriazine moiety forming M4 and M12 and subsequent glucuronide, sulfate, and glutathione conjugation reactions to afford M2, M10, and M11, respectively. The glutathione conjugate of TAK-041 (M11) undergoes extensive and sequential downstream metabolism to produce the cysteine S-conjugate (M1), which then undergoes *N*-acetylation to mercapturic acid (M3) and/or conversion to glutathione adduct–derived thiol metabolites to yield methylsulfone (M7), methylsulfide (M8), and methylsulfoxide (M9). Other metabolites including oxidative *N*-dealkylation at the carbon α to *N*-3 of the triazine-4-one moiety to form unstable carbinolamine followed by release of oxobenzotriazine moiety and subsequent reduction to form the corresponding alcohol cleaved product M5, hydroxylation on the trifluoromethoxy phenyl to form M6, novel ring closure and hydrolysis to form M13 were also tentatively identified. A proposed scheme for the biotransformation pathways of TAK-041 is shown in Fig. 11.

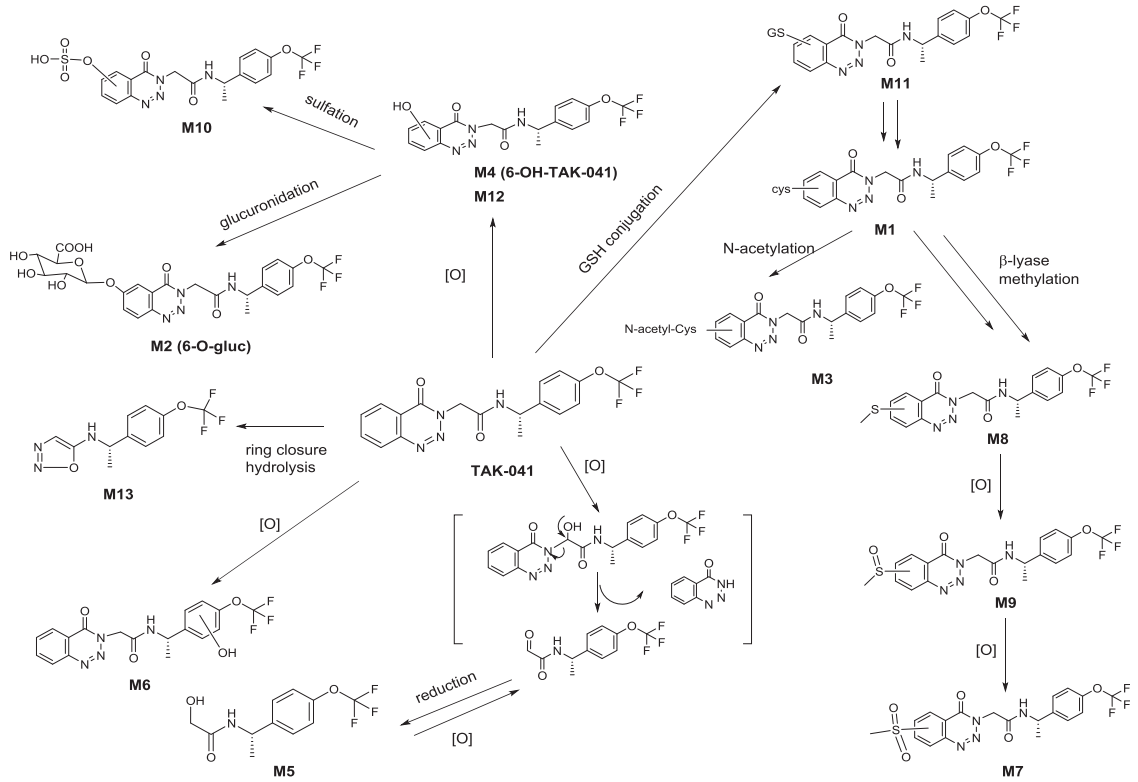

Fig. 11. Proposed biotransformation pathways of TAK-041 from in vitro incubation using the HepatoPac model. 6-O-gluc, 6-O-glucuronide.

The formation of M13 is probably initiated by delocalization of the amide nitrogen lone pair and attack of the amide oxygen on *N*-2 of the 4-oxo-benzotriazine moiety, ring formation, and addition of a proton to form the 2-imino-5-oxo-oxadiazolo-benzotriazine. Hydrolysis at the electron-deficient C-5 of the 5-oxo-benzotriazine moiety, subsequent ring scission, and release of aminobenzoic acid, followed by tautomeric conjugation of the double bond, leads to the formation of M13 as (*S*)-*N*-(1-(4-(trifluoromethoxy)phenyl)ethyl)-1,2,3-oxadiazol-5-amine. It is reasonable to assume that under the incubation conditions, the hydrolysis step proceeds via an enzymatic pathway and that base hydrolysis is unlikely. Although M13 may be found in both the imine and amine forms, it is likely that M13 exists predominantly in the more conjugated and energetically favorable amine form. The formation of M13 represented a minor metabolic pathway, so chemical synthesis was not warranted to unequivocally confirm its structure. A proposed mechanism for the formation of M13 is shown in Fig. 12.

A summary of TAK-041 observed metabolites and their description after incubation in rat, dog, monkey, and human hepatocyte suspension and HepatoPac model compared with in vivo circulating metabolites is presented in Tables 1–4, respectively. The HepatoPac model generated more robust metabolites and turnover over 14 days than those observed using traditional hepatocyte suspension. There were only a few metabolites detected after suspension hepatocyte incubations with TAK-041, whereas multiple metabolites were detected in the corresponding HepatoPac incubations including an extensive and unusual glutathione downstream metabolism to produce cysteine S-conjugate, *N*-acetylcysteine, and glutathione-derived thiol metabolites. This extensive downstream glutathione-derived thiol metabolites pathway is consistent with the fact that the glutathione conjugate (M11) was only detected in the early time point incubations (2, 4, 24, and 48 hours) and not in the 14-day incubation. An interesting finding was observed: in addition to human, dog MPCC hepatocytes appeared to produce a small amount of M3 (*N*-acetylcysteine conjugate), yet dogs are unable to acetylate xenobiotics because they lack *N*-acetyltransferase 2, the enzyme responsible for the biotransformation of cysteine S-conjugate to its mercapturic acid (Trepanier et al., 1997, Loureiro et al., 2013). The formation of M3 in dog MPCC hepatocytes could be attributed to the fact that the MCPP system uses human fibroblasts for dog matrix-coculture and is consistent with similar reported findings (Ballard et al., 2016).

The HepatoPac model was also investigated for cross-species comparison to determine any notable species difference in the rate and in the extent of its metabolic pathways and to establish correlation with in vivo metabolism. Results yielded good correlation between in vivo metabolites detected and in vitro MPCC hepatocyte metabolites across human and preclinical species (Tables 1–4). The qualitative cross-species MPCC metabolite profiles of TAK-041 generally agreed with clearance data displaying parent depletion in close agreement with in vivo half-life data across species, with dogs having the highest metabolic clearance and humans the slowest. The $t_{1/2}$ was ~3 hours in dog and ~11 days in human. Although several reports have been published demonstrating the utility of the HepatoPac model to study clearance prediction and multiple-step metabolism of slowly cleared compounds, our results, to the best of our knowledge, showed for the first time the suitability of the HeptaoPac model to study extensive and unusual downstream sequential metabolism of cysteine S-conjugate to thiol-derived metabolites via the β-lyase pathway in preclinical species and human.

In summary, the results of this study provide the first successful analysis of the formation of in vitro metabolites of slowly and extensively metabolized clinical candidate TAK-041 using the HepatoPac model when the hepatocyte suspension incubation was inadequate. Predominant metabolites correlated with relevant metabolites reported in human and preclinical species in vivo studies. The model also shows its suitability for species comparison and establishing correlation with in vivo metabolism in preclinical species and human. We have reported unusual glutathione

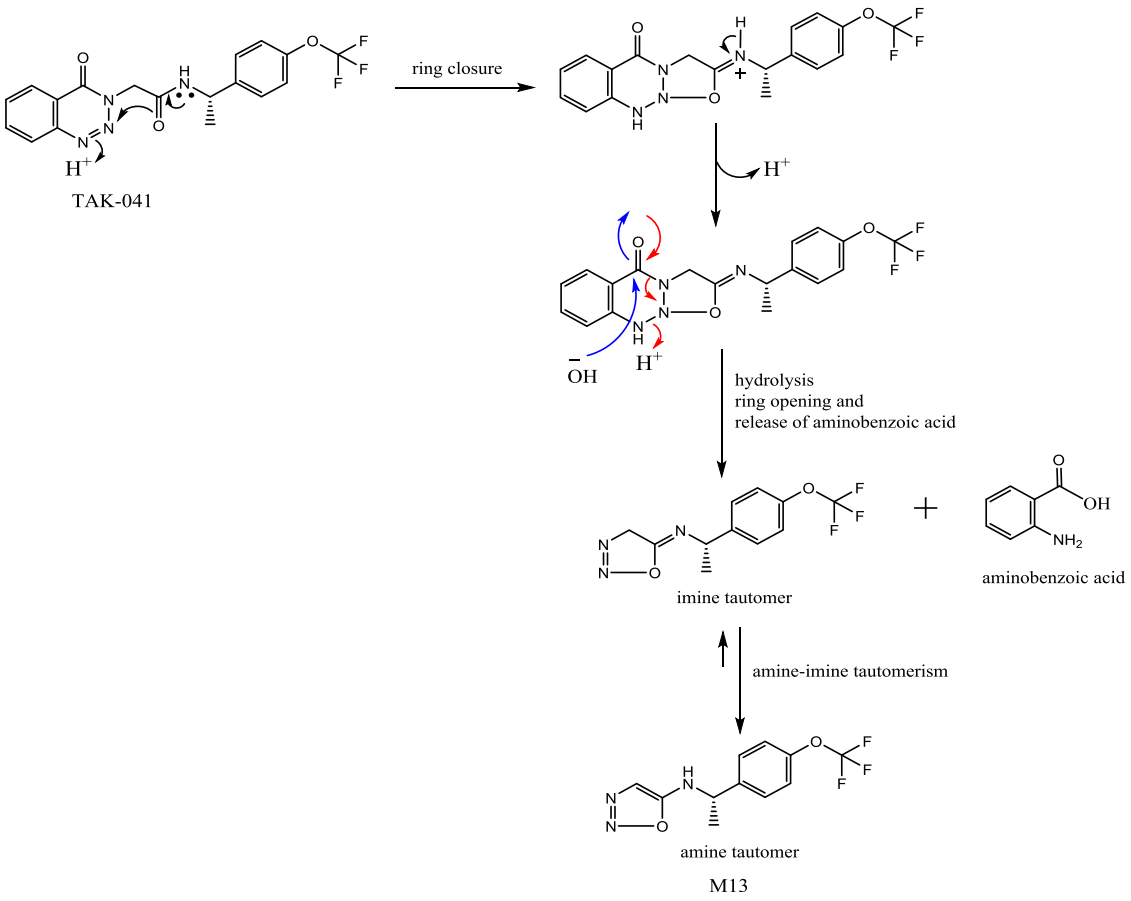

Fig. 12. Proposed mechanism for the formation of the oxadiazole amine metabolite M13.

extensive and sequential downstream metabolism affording the cysteine S-conjugate, which then undergoes *N*-acetylation to mercapturic acid and/or conversion to glutathione adduct–derived thiol metabolites via β-lyase pathway. We have also tentatively characterized a novel metabolite that results from ring closure and subsequent hydrolytic ring scission of the oxobenzotriazine moiety to form oxadiazole amine structure.

Acknowledgments

We thank Kirk Kozminski and Natalie Nguyen for help with hepatocyte suspension and HepatoPac incubations, Drs. Sean Murphy and Holly Reichard for synthesis of standards, Drs. Josh Johnson and Matt Russo for careful and critical reading of our manuscript, and Dr. Donavon McConn for helpful discussions.

Authorship Contributions

Participated in research design: Kamel, Bowlin.

Conducted experiments: Bowlin.

Performed data analysis: Kamel, Bowlin.

Wrote or contributed to the writing of the manuscript: Kamel, Bowlin, Hosea, Arkilo, Laurenza.

References

Alavi MS, Shamsizadeh A, Azhdari-Zarmehri H, and Roohbakhsh A (2018) Orphan G protein-coupled receptors: the role in CNS disorders. *Biomed Pharmacother* **98**:222–232.

Ballard TE, Wang S, Cox LM, Moen MA, Krzyzewski S, Ukairo O, and Obach RS (2016) Application of a micropatterned cocultured hepatocyte system to predict preclinical and human-specific drug metabolism. *Drug Metab Dispos* **44**:172–179.

Batalla A, Homberg JR, Lipina TV, Sescousse G, Luijten M, Ivanova SA, Schellekens AFA, and Loonen AJM (2017) The role of the habenula in the transition from reward to misery in substance use and mood disorders. *Neurosci Biobehav Rev* **80**:276–285.

Chan TS, Scaringella YS, Raymond K, and Taub ME (2020) Evaluation of erythromycin as a tool to assess CYP3A contribution of low clearance compounds in a long term hepatocyte culture. *Drug Metab Dispos* **48**:690–697.

Chan TS, Yu H, Moore A, Khetani SR, and Tweedie D (2019) Meeting the challenge of predicting hepatic clearance of compounds slowly metabolized by cytochrome P450 using a novel hepatocyte model, HepatoPac. *Drug Metab Dispos* **47**:58–66.

Docci L, Klammers F, Ekiciler A, Molitor B, Umehara K, Walter I, Krähenbühl S, Parrott N, and Fowler S (2020) In vitro to in vivo extrapolation of metabolic clearance for UGT substrates using short-term suspension and long-term co-cultured human hepatocytes [published correction appears in *AAPS J* (2020) 22:142]. *AAPS J* **22**:131.

Fowler CD and Kenny PJ (2012) Habenular signaling in nicotine reinforcement. *Neuropsychopharmacology* **37**:306–307.

Gloriam DE, Schiöth HB, and Fredriksson R (2005) Nine new human Rhodopsin family G-protein coupled receptors: identification, sequence characterisation and evolutionary relationship. *Biochim Biophys Acta* **1722**:235–246.

Gómez-Lechón MJ, Castell JV, and Donato MT (2008) An update on metabolism studies using human hepatocytes in primary culture. *Expert Opin Drug Metab Toxicol* **4**:837–854.

Hamilton RA, Garnett WR, and Kline BJ (1981) Determination of mean valproic acid serum level by assay of a single pooled sample. *Clin Pharmacol Ther* **29**:408–413.

Hitchcock S, Lam B, Monenschein H, and Reichard H (2016) inventors. 4-oxo-3,4-dihydro-1,2,3-benzotriazines as modulators of GPR139. Patent WO/2016/081736. 2016 May 26.

Hutzler JM, Ring BJ, and Anderson SR (2015) Low-turnover drug molecules: a current challenge for drug metabolism scientists. *Drug Metab Dispos* **43**:1917–1928.

Loureiro AI, Fernandes-Lopes C, Bonifácio MJ, Wright LC, and Soares-da-Silva P (2013) N-acetylation of etamicastat, a reversible dopamine-β-hydroxylase inhibitor. *Drug Metab Dispos* **41**:2081–2086.

Matsuo A, Matsumoto S, Nagano M, Masumoto KH, Takasaki J, Matsumoto M, Kobori M, Katoh M, and Shigeyoshi Y (2005) Molecular cloning and characterization of a novel Gq-coupled orphan receptor GPRg1 exclusively expressed in the central nervous system. *Biochem Biophys Res Commun* **331**:363–369.

Ramsden D, Tweedie DJ, St George R, Chen L-Z, and Li Y (2014) Generating an in vitro-in vivo correlation for metabolism and liver enrichment of a hepatitis C virus drug, faldaprevir, using a rat hepatocyte model (HepatoPac). *Drug Metab Dispos* **42**:407–414.

Trepanier LA, Ray K, Winand NJ, Spielberg SP, and Cribb AE (1997) Cytosolic arylamine N-acetyltransferase (NAT) deficiency in the dog and other canids due to an absence of NAT genes. *Biochem Pharmacol* **54**:73–80.

Wang J, Zhu LY, Liu Q, Hentzer M, Smith GP, and Wang MW (2015) High-throughput screening of antagonists for the orphan G-protein coupled receptor GPR139. *Acta Pharmacol Sin* **36**:874–878.

Address correspondence to: Dr. Amin Kamel, Global Drug Metabolism and Pharmacokinetics, Takeda California Inc., 9625 Towne Center Dr., San Diego, CA 92121. E-mail: Amin.kamel@takeda.com